

Isotopic and kinetic assessment of the mechanism of methane reforming and decomposition reactions on supported iridium catalysts

Junmei Wei and Enrique Iglesia*

Department of Chemical Engineering, University of California at Berkeley, Berkeley, CA 94720.
E-mail: iglesias@cchem.berkeley.edu; Fax: (510)642-4778; Tel: (510)-642-9673

Received 20th January 2004, Accepted 19th March 2004
First published as an Advance Article on the web 26th April 2004

Isotopic tracer and kinetic measurements were used to determine the identity and reversibility of elementary steps required for CH₄-CO₂, CH₄-H₂O and CH₄ decomposition reactions on supported Ir clusters. The results led to a simple and rigorous mechanism that includes steps required for these reactions as well as water-gas shift reactions. All three CH₄ reactions gave similar forward rates, rate constants, activation energies, and kinetic isotopic effects, indicating that C-H bond activation is the only kinetically relevant step on Ir surfaces. CO₂ and H₂O activation is quasi-equilibrated and intermediates derived from these co-reactants are not involved in kinetically-relevant steps. Isotopic cross-exchange during CH₄/CD₄/CO₂ and CH₄/CD₄/H₂O reactions is much slower than chemical conversion, indicating that C-H bond activation is irreversible. Identical ¹³C contents in CO and CO₂ formed from ¹²CH₄/¹²CO₂/¹³CO reactions showed that CO₂ activation is reversible and quasi-equilibrated. Binomial isotopomer distributions in water and dihydrogen formed from CH₄/CO₂/D₂ and CD₄/H₂O mixtures are consistent with quasi-equilibrated hydrogen and water activation and recombinative desorption during CH₄ reforming on Ir surfaces. Taken together with the quasi-equilibrated nature of CO₂ activation steps, these data require that water-gas shift reactions must also be at equilibrium, as confirmed by analysis of the products formed in CH₄ reforming reactions.

1. Introduction

Methane is an essential raw material in the synthesis of liquid fuels and petrochemical, but its strong C-H bonds (439 kJ mol⁻¹) require active catalysts and severe reaction conditions to overcome kinetic and thermodynamic hurdles. Supported Ir clusters activate C-H bond at high temperatures without significant sintering or carbon formation²⁻⁴ and with turnover rates higher than on any other noble metals except Pt.⁵ Experimental and theoretical studies of C-H bond activation on Ir single crystals have shown that coordinatively unsaturated surface atoms lead to higher CH₄ dissociation rates than atoms on closed-packed surfaces.⁶⁻⁸

Recently, we have reported some kinetic evidence for the rate-limiting nature of C-H bond activation steps during CH₄ reactions with CO₂ or H₂O and for CH₄ decomposition.⁹ The surfaces of Ir clusters remained largely uncovered by reactive intermediates or unreactive carbon during steady-state reforming reactions, because co-reactant activation and their reactions with CH₄-derived chemisorbed carbon species are more facile than C-H bond activation steps; as a result, CH₄ reforming turnover rates do not depend on the concentration or the identity of the co-reactants (H₂O or CO₂) or on the nature of the support (Al₂O₃, ZrO₂).⁹ C-H bond activation rate constants, and therefore CH₄ reforming turnover rates, increased markedly with increasing dispersion of Ir clusters, apparently as a result of the higher reactivity of the coordinatively unsaturated surface atoms prevalent in smaller metal clusters.⁹

These previous findings provided a unifying mechanistic picture of reforming and related reactions of CH₄ and led us to propose a set of required elementary steps, initially based on the dependence of rates on CH₄ and co-reactant concentrations. Here, we present more rigorous evidence for the identity and reversibility of the elementary steps required for H₂O and CO₂ reforming on Ir clusters using isotopic studies. We also

establish a rigorous kinetic and mechanistic connection among water-gas shift, CH₄ decomposition, and CO₂ and H₂O reforming reactions, which are typically, but non-rigorously, treated as kinetically independent events. The mechanistic conclusions reached and the identity and kinetic relevance of various elementary steps are in agreement with those reported in previous studies on Pt,⁵ Rh,¹⁰ Ru¹¹ and Ni.¹²

2. Experimental

Ir/ZrO₂ (0.8 and 1.6 wt.% Ir) samples were prepared by incipient wetness impregnation of ZrO₂ with aqueous IrCl₃·3H₂O solutions (Aldrich, 99%) followed by drying in ambient air at 393 K and treatment in flowing dry air (Airgas, UHP, 1.2 cm³ g⁻¹ s⁻¹) at 873 K (0.167 K s⁻¹) for 5 h. Samples were then treated in flowing H₂ (Airgas, UHP, 50 cm³ g⁻¹ s⁻¹) by raising the temperature to 873 K at 0.167 K s⁻¹ and holding for 2 h. The ZrO₂ support (45 m² g⁻¹) was prepared using previously reported procedures.¹² Ir dispersion was measured using volumetric uptakes of strongly chemisorbed hydrogen at 313 K.¹¹ Fractional Ir dispersions were 0.52 and 0.42 for the 0.8 and 1.6 wt.% Ir samples, respectively, assuming a 1:1 H:Ir stoichiometry.¹³

Reaction rates were measured on pellets (diameter: 250–425 μm) consisting of 5 mg catalyst and 25 mg Al₂O₃ held within a high-pressure packed-bed microreactor.^{11,12} These pellets were further diluted with 500 mg acid-washed quartz of similar size in order to avoid temperature and concentration gradients. Reactants consisted of 50% CH₄/Ar (Matheson) and 50% CO₂/Ar (Matheson) certified mixtures with He (Airgas, UHP) as a diluent. H₂O was introduced with a syringe pump (Cole-Parmer, 74900 series) through transfer lines kept above 373 K to avoid condensation. CH₄ and CO₂ pressure effects on rates of CH₄ reactions with CO₂ were measured at 823–1023 K and 100–1000 kPa total pressure over a wide range of reactant

ratios. H₂O pressure effects on steam reforming rates were measured at 823–1023 K and 100 kPa total pressure.

Kinetic isotope effects were measured from reaction rates with CH₄/CO₂ and CD₄(Isotec, chemical purity >99.0%)/CO₂ reactant mixtures for CO₂ reforming reactions and with CH₄/H₂O, CD₄/H₂O, and CD₄/D₂O (Cambridge Isotope Laboratories, Inc. chemical purity: 99.9%) mixtures for steam reforming. Effluent concentrations were determined by gas chromatography (Hewlett-Packard Model 6890 GC; Carboxen 1000 (3.2 mm × 2 m) packed column) using thermal conductivity detector.

Ir/ZrO₂ (0.8 wt.%, 20 mg; diluted with 500 mg quartz) was used to measure rates of CH₄ and CD₄ decomposition (without co-reactants) at 873 K using on-line mass spectrometry (Leybold Inficon, Transpector Series; 15 and 18 amu intensities). Reactants (20% CH₄/Ar or 20% CD₄/Ar) were prepared using 50% CH₄/Ar (Matheson, certified mixture) or pure CD₄ and Ar (Airgas, UHP). Methane decomposition rates extrapolated to zero reaction time were used to obtain rate constants, based on the observed linear dependence of rates on CH₄ partial pressures.

Isotopic tracer studies of CH₄ reforming reactions were carried out on 1.6 wt.% Ir/ZrO₂ using a transient flow apparatus with short hydrodynamic delays (<5 s). Chemical and isotopic compositions were measured using on-line mass spectrometry (Leybold Inficon, Transpector Series). CD₄, D₂O (Isotec, chemical purity >99.0%), 5% D₂/Ar and ¹³CO (Isotec, chemical purity >99.0%) were used as reactants without further purification. Intensities at 15 and 17–20 amu were used to measure methane isotopomer concentrations. Intensities at 18–20 amu were used to determine water isotopomers and those at 28, 29, 44, and 45 amu to measure ¹²CO, ¹³CO, ¹²CO₂, and ¹³CO₂ concentrations, respectively.

3. Results and discussion

3.1. Kinetic measurements for CH₄ reactions

The kinetic dependences of forward CH₄ reaction rates on CH₄, CO₂ or H₂O pressures were studied on 0.8 wt.% Ir/ZrO₂. The absence of transport artifacts was confirmed by the same CH₄ reaction rates measured using different intrapellet dilution ratios (5:1 and 10:1 within the pellet) and pellet sizes (63–106 and 250–425 μm) (Fig. 1). Fig. 2 shows the effects of CH₄ (10–300 kPa, Fig. 2a) and CO₂ pressures (10–300 kPa,

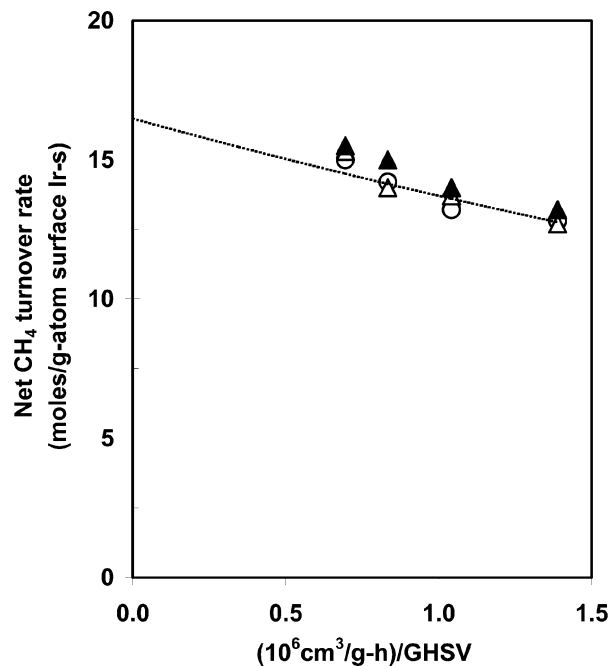


Fig. 1 Net CH₄ reaction rates versus residence time for CH₄-CO₂ reaction on 0.8 wt.% Ir/ZrO₂ [873 K, (▲) 5 mg catalyst diluted with 50 mg Al₂O₃ within pellets, then diluted with 500 mg ground quartz, pellet size 250–425 μm; (○) 5 mg catalyst diluted with 25 mg Al₂O₃ within pellets, then diluted with 500 mg ground quartz, pellet size 250–425 μm; (△) 5 mg catalyst diluted with 25 mg Al₂O₃ within pellets, then diluted with 500 mg ground quartz, pellet size 63–106 μm, The dash line extrapolated to zero residence time gives forward CH₄ reaction rate].

Fig. 2b) on forward CH₄ reaction rate (r_f) for CO₂/CH₄ reactions on 0.8 wt.% Ir/ZrO₂ at 873 K. CH₄ and H₂O pressure effects on forward CH₄ reaction rates with H₂O/CH₄ reactants are also shown in Fig. 2. The reversible nature of endothermic reforming reactions requires that we rigorously correct measured net reaction rates (r_n) (normalized by exposed Ir atoms) by their approach to equilibrium to obtain kinetic rates reflecting only the forward reaction. Forward reforming rates are obtained from measured net rates using:

$$r_n = (r_f - r_r) = r_f(1 - \eta). \quad (1)$$

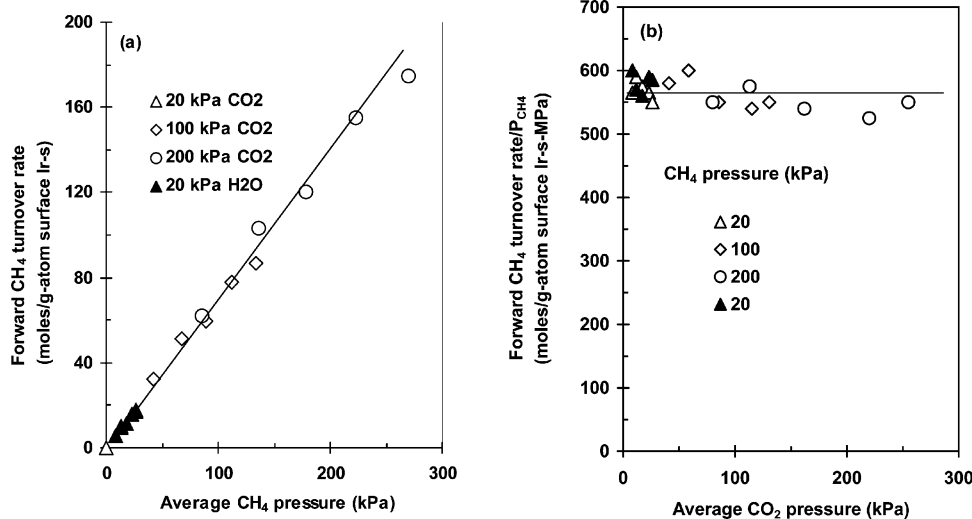


Fig. 2 Effects of CH₄ (a) and CO₂ or H₂O (b) pressure on forward CH₄ turnover rate for CH₄-CO₂ (open symbol) and CH₄-H₂O (solid symbol) reaction on 0.8 wt.% Ir/ZrO₂ (873 K, balance He, average pressure is the average of inlet and outlet pressures within the reactor, these figures are modified from Fig. 1 in ref. 9).

in which the approach to equilibrium η is given by:

$$\eta_1 = \frac{[P_{\text{CO}}]^2 [P_{\text{H}_2}]^2}{[P_{\text{CH}_4}] [P_{\text{CO}_2}]} \times \frac{1}{K_1} \quad (2)$$

and

$$\eta_2 = \frac{[P_{\text{CO}}] [P_{\text{H}_2}]^3}{[P_{\text{CH}_4}] [P_{\text{H}_2\text{O}}]} \times \frac{1}{K_2} \quad (3)$$

for CO_2/CH_4 and $\text{H}_2\text{O}/\text{CH}_4$ reactions, respectively.^{10–12} $[P_j]$ represents average partial pressures of species j (in atm) within the catalyst bed for a given set of conditions; they are used to correct for minor reactant depletion along the bed. K_1 and K_2 are equilibrium constants for each reaction.¹⁴

Forward reforming rates are proportional to CH_4 pressure (Fig. 2a) and independent of CO_2 pressures (Fig. 2b) throughout the range of pressures examined (100–1000 kPa total pressures). Similarly, reactions of $\text{CH}_4\text{--H}_2\text{O}$ mixtures exhibit a first order dependence on CH_4 pressure and their rates do not depend on H_2O pressures. The addition of H_2 or CO to $\text{CH}_4\text{--H}_2\text{O}$ or $\text{CH}_4\text{--CO}_2$ reactants decreased net rates, but not forward reaction rates, indicating that they influence the approach to equilibrium but not CH_4 reforming kinetics.⁹ Chemical analyses of the reactants and products indicated that water–gas shift reactions are at equilibrium during CH_4 reforming reactions, as shown by the data in Fig. 3. Thus, CO_2/CH_4 and $\text{H}_2\text{O}/\text{CH}_4$ reaction rates are simply described by the rate expression

$$r_f = kP_{\text{CH}_4}. \quad (4)$$

Forward CH_4 reaction rates for H_2O and CO_2 are not only independent of the concentration of the co-reactants, but also of their identity (Fig. 2) and the rate constant k in eqn. (4) is the same for steam and CO_2 reforming reactions (Table 1). Reforming rates are also similar to those measured during the initial stages of CH_4 decomposition on each Ir catalyst (Table 1). Similar rate constants were also measured for both CH_4 reforming reactions and for CH_4 decomposition at other reaction temperatures (823–973 K), indicating that activation energies for CO_2 (86 kJ mol⁻¹) and H_2O (87 kJ mol⁻¹)

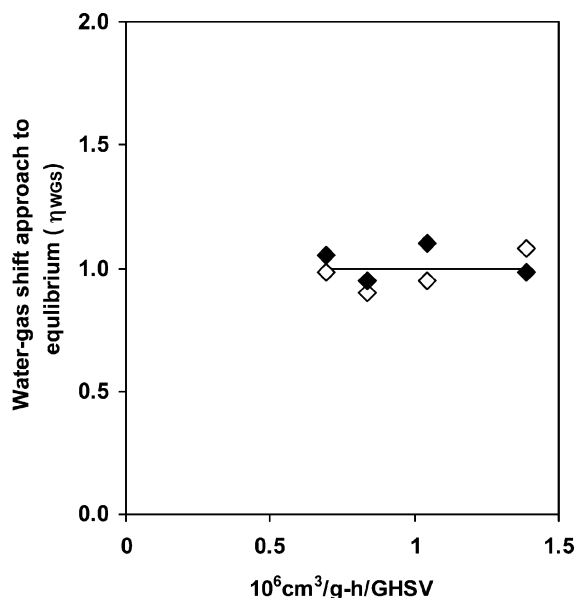


Fig. 3 Water–gas–shift approach to equilibrium as a function of space velocity at 873 K for CH_4/CO_2 (◆) and $\text{CH}_4/\text{H}_2\text{O}$ (◇) reactions on 0.8 wt.% Ir/ ZrO_2 (reaction conditions: 25 kPa CO_2 or H_2O , 25 kPa CH_4 , 100 kPa total pressure, balance Ar, $\eta_{\text{WGS}} = ([P_{\text{CO}}] [P_{\text{H}_2\text{O}}]) / ([P_{\text{H}_2}] [P_{\text{CO}_2}] K_{\text{WGS}})$).

Table 1 Forward CH_4 turnover rates, rate constants, activation energies, and kinetic isotopic effect (KIE) for CH_4 reactions on 0.8 wt.% Ir/ ZrO_2 (873 K, 20 kPa CH_4 or CD_4 , 25 kPa CO_2 or H_2O , balance Ar)

Co-reactant	Turnover rate/s ⁻¹	Rate constant/s ⁻¹ kPa ⁻¹	Activation energy/kJ mol ⁻¹	KIE
CO_2	13.0	0.65	86 ± 5	1.75
H_2O	12.4	0.62	87 ± 3	1.81
None	11.2 ^a	0.56	81 ± 6	1.68

^a Initial CH_4 decomposition rate.

reforming and for CH_4 decomposition (81 kJ mol⁻¹) are also similar (Table 1). These activation energies resemble those reported previously for CO_2 reforming on Ir catalysts (103 kJ mol⁻¹ on Ir/MgO;¹⁵ 85 kJ mol⁻¹ on Ir/ TiO_2 ¹⁶). These activation energies are much larger than the values of 29 kJ mol⁻¹¹⁷ and 28 kJ mol⁻¹¹⁸ reported for dissociative chemisorption of CH_4 in molecular beam studies on Ir(110) and Ir(111), respectively, in agreement with density functional theory estimates of 30 kJ mol⁻¹ for activation of CH_4 on Ir(111).⁶ The origins of these differences remain unclear; they may reflect the presence of very reactive minority sites that do not turnover because they form irreversibly chemisorbed carbon^{9–12} or the reported surface melting of small metal clusters at reforming temperatures (800–1100 K),^{19,20} which precludes coordinative unsaturation, a property leading to fast C–H bond activation and otherwise expected in small clusters. These differences between surface reactivity for CH_4 reactions on single crystals and on small clusters have been observed on Pt,⁵ Rh¹⁰ and Ru,¹¹ and Ni¹² clusters; they indicate that large oriented crystals fail to describe some essential features relevant to catalysis on small metal clusters.

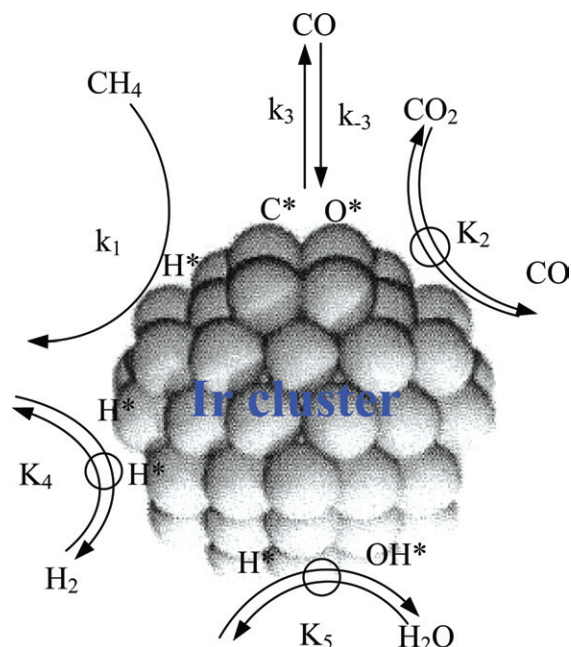
These similarities in rates, rate constants, and activation energies for H_2O and CO_2 reforming and decomposition reactions indicate the involvement of a common kinetically-relevant step. This insensitivity to co-reactant concentration and identity indicates that this step does not involve reactive intermediates derived from co-reactants and the number of unoccupied sites available for this step is unaffected by co-reactants, indicating also that all reactive intermediates are present at low coverages during steady-state catalysis. Co-reactants are required by stoichiometry, but their activation or subsequent reactions are not kinetically relevant.

3.2. CH_4/CD_4 kinetic isotope effects for reforming and decomposition reactions

Similar kinetic isotope effects measured for these three reactions confirmed that C–H bond activation is the sole kinetically-relevant step (Table 1). CO_2 reforming kinetic isotope effects were measured on 0.8 wt.% Ir/ ZrO_2 from forward rates of $\text{CH}_4\text{--CO}_2$ and $\text{CD}_4\text{--CO}_2$ mixtures at 873 K. H_2O reforming kinetic isotope effects were obtained from the corresponding forward rates for $\text{CD}_4\text{--H}_2\text{O}$ and $\text{CD}_4\text{--D}_2\text{O}$ reactants at 873 K. The kinetic isotope effects for CO_2 reforming (1.75) were similar to those measured for H_2O reforming (1.81) within experimental accuracy. These kinetic isotope effects are also similar to those measured for methane decomposition (1.68) from initial CH_4 and CD_4 decomposition rates. The lack of kinetic relevance for steps involving water-derived intermediates is apparent from the similar reaction rates measured for $\text{CD}_4\text{--H}_2\text{O}$ and $\text{CD}_4\text{--D}_2\text{O}$ reactants (KIE: 1.05).

3.3. Elementary steps involved in CH_4 reactions

The apparent kinetic equivalence among these CH_4 reactions leads us to propose a common sequence of elementary steps for reactions of CH_4 with CO_2 or H_2O on Ir clusters



Scheme 1 Sequence of elementary steps for CH₄ reforming and water–gas shift reactions on Ir clusters (→ irreversible step, \rightleftharpoons quasi-equilibrated step, \rightleftharpoons reversible step, k_i is the rate coefficient and K_i is the equilibrium constant for a given step i).

(Scheme 1). This network also contains all the necessary steps for CH₄ decomposition and water–gas shift reactions. CH₄ dissociates in a series of irreversible steps to form ultimately chemisorbed carbon (C*); these steps become faster as H-atoms are sequentially abstracted.⁸ CO₂ and H₂O are dissociatively adsorbed in quasi-equilibrated steps that form chemisorbed oxygen, which reacts with C* to form adsorbed CO; CO then desorbs along with the H-atoms formed in C–H activation *via* equilibrated recombinative desorption steps. These elementary steps are similar to those proposed and found relevant to reactions of CH₄ on Pt,⁵ Rh¹⁰ and Ru¹¹ and Ni¹² surfaces. The identity and reversibility of these elementary steps are probed next using isotopic tracer and exchange methods.

3.4. Isotopic tracer studies of the reversibility of C–H bond activation

If C–H bond activation is the only kinetically-relevant step, this step must be exactly as reversible as the overall CH₄ reforming reaction, as shown by non-equilibrium thermodynamic treatments of catalytic sequences.²¹ The reversibility of C–H bond activation steps can be probed from the relative rates of chemical conversion and of isotopic cross-exchange with CH₄/CD₄/CO₂ (1:1:2) reactant mixtures during CO₂ reforming reactions at 873 K and with CH₄/CD₄/H₂O (1:1:2) reactant mixtures during H₂O reforming reactions at 873–973 K. These rates were measured by on-line mass spectrometry after removing H_xD_{2-x}O at 218 K to avoid interference among H₂O, HDO, D₂O mass fragments and those for CH_{4-x}D_x. The formation rates of different methane isotopomers and the methane chemical conversion rates during CO₂ reforming are shown in Fig. 4; the corresponding results for H₂O reforming are shown in Table 2.

CH₄/CD₄ cross exchange turnover rates, defined as the sum of the rates of formation of CHD₃, CH₂D₂ (taken twice) and CH₃D, is 0.9 s⁻¹, the methane chemical conversion rate is 9.4 s⁻¹ during the reaction of CH₄/CD₄/CO₂ (1:1:2) mixtures, indicating that ratio of the recombination rate to that of chemical conversion is 0.09. The approach to equilibrium for this

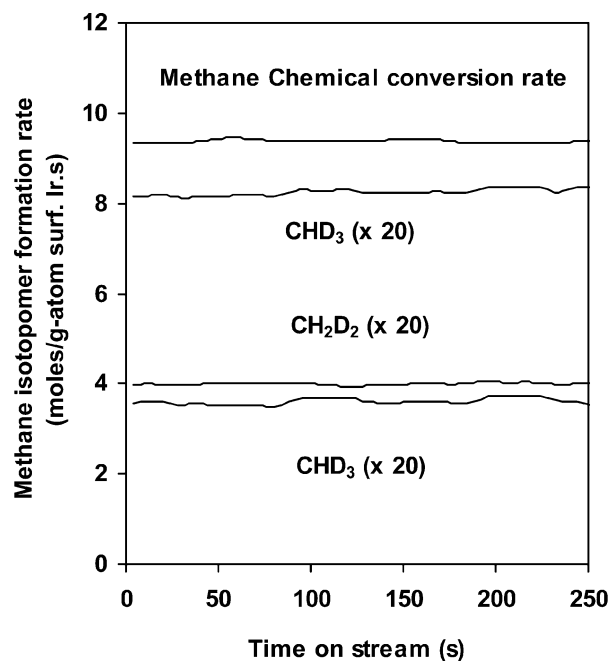


Fig. 4 Methane turnover rates and CH₄/CD₄ cross exchange rates during the reaction of CH₄/CD₄/CO₂ mixture on 1.6 wt.% Ir/ZrO₂ catalyst (3 mg catalyst, 873 K, 12.5 kPa CH₄ and CD₄, 25 kPa CO₂, 100 kPa total pressure, balance Ar).

reaction, η , estimated from the prevalent concentrations of all reactants and products is 0.08, corresponding to a ratio of forward to reverse reaction rates of 12, indicating that CHD₃, CH₂D₂ and CH₃D isotopomers formed merely because the overall reaction is reversible to some extent at the conditions of the experiment. These experiments also showed that the ratio of CH₄ and CD₄ reaction rates is 1.71 during CH₄/CD₄/CO₂ (1:1:2) reactions at 873 K; this ratio is consistent with the kinetic isotope effects measured independently from CH₄–CO₂ and CD₄–CO₂ reactants (1.75).

Methane chemical conversion and CH₄/CD₄ cross exchange rates during reaction of CH₄/CD₄/H₂O mixtures on 1.6 wt.% Ir/ZrO₂ led to similar conclusions about the irreversible nature of C–H bond activation steps during steam reforming reactions at 873–973 K (Table 2). Cross-exchange to chemical conversion rate ratios were 0.09–0.11 and similar to those predicted from the reversibility of the overall steam reforming reactions.

Table 2 Methane chemical conversion and CH₄/CD₄ cross exchange rates during reaction of CH₄/CD₄/H₂O mixture on 3 mg 1.6 wt.% Ir/ZrO₂ (12.5 kPa CH₄, 12.5 kPa CD₄, 25 kPa H₂O, 100 kPa total pressure, balance Ar)

Reaction temperature/K	Methane chemical conversion rate/s ⁻¹ ^a	Cross exchange rate/s ⁻¹ ^b	$r_{\text{exch}}/r_{\text{reaction}}$ ^c	η ^d
873	9.0	0.8	0.09	0.07
923	16.5	1.7	0.10	0.06
973	27.8	3.1	0.11	0.09

^a Forward methane chemical conversion rate. ^b Total methane isotopomers formation rate. ^c Ratio of total methane isotopomers formation rate to the methane chemical conversion rate. ^d $\eta = ([P_{\text{CO}}][P_{\text{H}_2}]^3)/([P_{\text{H}_2\text{O}}][P_{\text{CH}_4}]K)$; approach to equilibrium for H₂O reforming reaction.

3.5. Isotopic tracer studies of the reversibility of H₂O and H₂ formation

H₂, HD and D₂ molecules formed from CH₄/CD₄/CO₂ mixtures in the reactions described in the previous section showed a binomial isotopomer distribution, indicating that recombinative hydrogen desorption steps are quasi-equilibrated. This finding was confirmed by independent measurements of the dihydrogen isotopomer distribution obtained from reactions of CH₄/CO₂/D₂ (1:1:0.2) mixtures on 1.6 wt.% Ir/ZrO₂. Dihydrogen isotopomers were measured by on-line mass spectrometry during reactions of CH₄/CO₂/D₂ (1:1:0.2) mixtures on 1.6 wt.% Ir/ZrO₂ at 873 K. The H/D fraction expected if all H-atoms in chemically converted CH₄ molecules and all D-atoms in D₂ molecules contributed to the pool of surface intermediates forming water and dihydrogen is 0.90. The measured H/D ratio in dihydrogen molecules was 0.92 and the isotopomer distribution was binomial (Fig. 5). Thus, H* recombinative desorption steps to form dihydrogen molecules is reversible and quasi-equilibrated during CO₂ reforming reactions. The distribution of water isotopomers (H₂O, HDO and D₂O) was also binomial and its H/D fraction was 0.87, as expected from the hydrogen pool composition and from the H/D ratio measured in dihydrogen isotopomers. These data indicate that all steps involved in water formation or water activation are also reversible and quasi-equilibrated during CH₄ reforming reactions.

The quasi-equilibrated nature of H₂O activation and H₂ formation during steam reforming reactions was confirmed from the water and dihydrogen isotopomers formed from CD₄/H₂O (1:1) reactant mixtures on 1.6 wt.% Ir/ZrO₂ at 873 K. The D/H fraction expected if all D-atoms in chemically converted CD₄ molecules and all H-atoms in H₂O reactant molecules contributed to the pool of surface intermediates is 0.16. The measured D/H ratio in water molecules was 0.13 and the isotopomer (H₂O, HDO and D₂O) distribution was binomial, indicating that H₂O activation steps during CH₄/H₂O reaction are reversible and quasi-equilibrated. In fact, all H₂O reactant molecules exchange rapidly with all D-atoms formed in C–D activation reactions of CD₄. The D/H ratio in dihydrogen molecules was 0.15, and binomial isotopomer distributions

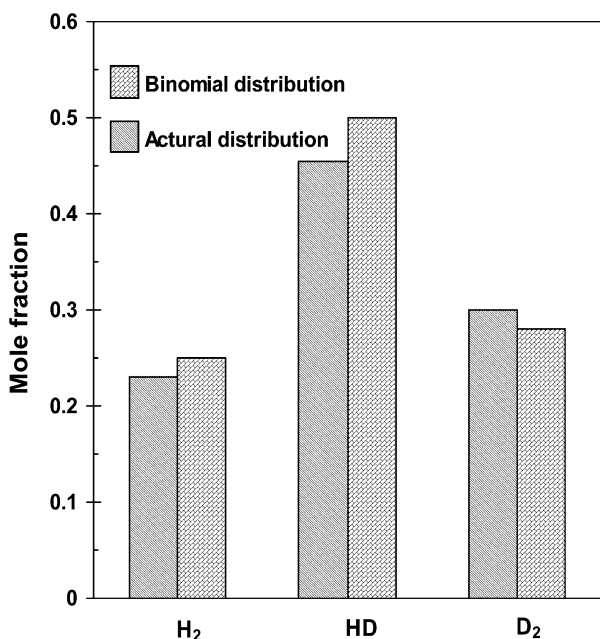


Fig. 5 Distribution of dihydrogen isotopomers during reactions of CH₄/CO₂/D₂ mixtures on 1.6 wt.% Ir/ZrO₂ (3 mg catalyst, 873 K, 16.7 kPa CH₄, 16.7 kPa CO₂, 3.3 kPa D₂, 100 kPa total pressure, balance Ar).

were observed, indicating that hydrogen recombinative desorption steps are reversible and quasi-equilibrated during steam reforming reactions on Ir clusters.

3.6. Isotopic tracer studies of the reversibility of CO₂ activation

The reversibility of CO₂ activation steps was probed during CO₂–CH₄ reactions using ¹²CH₄/¹²CO₂/¹³CO (1:1:0.4) reactant mixtures on 1.6 wt.% Ir/ZrO₂ at 873 K. Measured ¹³C fractions were very similar in the CO (0.26) and CO₂ (0.25) molecules present in the reactor effluent, even when overall reforming reactions were far from equilibrium ($\eta = 0.11$). These ¹³C contents reflect complete chemical and isotopic equilibration between CO and CO₂ molecules in the contacting gas phase; these data show that CO₂ dissociation to form CO and oxygen occurs in both directions many times during each CH₄ chemical conversion turnover. Thus, CO₂ activation steps are reversible and quasi-equilibrated during CH₄–CO₂ reactions.

The reversible CO₂ dissociation, CO desorption, and H₂ and H₂O formation steps in our proposed sequence combine to give a complete catalytic sequence for water–gas shift reactions. These individual steps are quasi-equilibrated; thus, overall water–gas shift reactions must also be quasi-equilibrated during CH₄ reforming reactions, as indeed found at all reaction conditions in this study (Fig. 3).

The reversibility of only one step in the proposed sequence (Scheme 1) remains undemonstrated. The reversibility of CO formation steps from adsorbed C* and O* (C* + O* → CO + 2*) during CH₄ reforming reactions will be examined in future studies by ¹⁸O and ¹³C isotopic tracing using ¹²CH₄/H₂¹⁶O/¹²C¹⁶O/¹³C¹⁸O/ reactant mixtures. The rate of formation of the mixed CO isotopomer (¹²C¹⁸O) relative to that of chemical conversion of CH₄ will demonstrate the reversibility of CO dissociation steps.

4. Conclusions

Isotopic tracer studies and kinetic measurements of forward rates uncorrupted by transport artifacts led to a simple and rigorous mechanistic picture containing pathways for CH₄–CO₂, CH₄–H₂O, CH₄ decomposition reactions and for water–gas shift on Ir cluster surfaces. The rates of these three CH₄ reactions are controlled only by the activation of C–H bonds in CH₄. Reaction rates, first-order rate constants, activation energies, and kinetic isotope effects are independent of the identity and concentration of co-reactants. CD₄/H₂O and CH₄/H₂O reactant mixtures gave similar rates; thus kinetically-relevant steps do not involve water or water-derived reactive intermediates. Chemical conversion of methane was much faster than isotopic cross-exchange among methane molecules during reactions of CH₄/CD₄/CO₂ or CH₄/CD₄/H₂O mixtures, indicating that kinetically relevant C–H bond activation steps are essentially irreversible. The identical ¹³C contents measured in CO and CO₂ during reactions of CH₄/CO₂/¹³CO mixtures showed that co-reactant activation steps are reversible and quasi-equilibrated. Dihydrogen and water molecules formed from CH₄/CO₂/D₂ mixtures contained the H/D ratios expected from complete equilibration between all D-atoms in D₂ and all H-atoms in reacted CH₄ and isotopomer distributions were binomial. Thus, recombinative desorption steps leading to water and dihydrogen were reversible and quasi-equilibrated during CO₂ reforming. Similar conclusions were reached for steam reforming reactions from the D-content and isotopomer distributions in the water and dihydrogen formed from CD₄–H₂O mixtures. The quasi-equilibrated nature of steps involving CO, CO₂, H₂, and H₂O requires that the water–gas shift reaction be at equilibrium during methane reforming reactions, as indeed found from the chemical

composition of reaction products formed at all conditions in this study.

Acknowledgements

This study was supported by BP as part of the Methane Conversion Cooperative Research Program at the University of California at Berkeley. Helpful technical discussions with Dr Theo Fleisch (BP) throughout these studies are gratefully acknowledged.

References

- 1 S. J. Blanksby and G. B. Ellison, *Acc. Chem. Res.*, 2003, **36**, 255.
- 2 M. F. Mark and W. F. Maier, *J. Catal.*, 1996, **164**, 122.
- 3 J. R. Rostrup-Nielsen and J. H. Bak Hansen, *J. Catal.*, 1993, **144**, 38.
- 4 A. T. Ashcroft, A. K. Cheetham, M. L. H. Green and P. D. F. Vernon, *Nature (London)*, 1991, **352**, 225.
- 5 J. Wei and E. Iglesia, *J. Phys. Chem.*, 2004, **108**, 4094.
- 6 G. Henkelman and H. Jonsson, *Phys. Rev. Lett.*, 2001, **86**, 664.
- 7 R. W. Verhoef, D. Kelly, C. B. Mullins and W. H. Weinberg, *Surf. Sci.*, 1995, **325**, 102.
- 8 H. Burghgraef, A. P. J. Janson and R. A. van Santen, *Surf. Sci.*, 1995, **324**, 345.
- 9 J. Wei and E. Iglesia, *Angew. Chem. Int. Edn.*, in press.
- 10 J. Wei and E. Iglesia, *J. Catal.*, in press.
- 11 J. Wei and E. Iglesia, *J. Phys. Chem.*, in press.
- 12 J. Wei and E. Iglesia, *J. Catal.*, in press.
- 13 O. S. Alexeev, D. W. Kim and B. C. Gates, *J. Mol. Catal. A*, 2000, **162**, 67.
- 14 D. R. Stull, F. Edgar, J. Westrum and G. C. Sinke, *The Thermodynamics of Organic Compounds*, Robert E. Krieger Publishing Co., Malabar, Florida, 1987.
- 15 D. Qin and J. Lapszewicz, *Catal. Today*, 1994, **21**, 551.
- 16 M. C. J. Bradford and M. A. Vannice, *Catal. Today*, 1999, **50**, 87.
- 17 R. W. Verhoef, D. Kelly, C. B. Mullins and W. H. Weinberg, *Surf. Sci.*, 1993, **287**, 94.
- 18 D. C. Seets, C. T. Reeves, B. A. Ferguson, M. C. Wheeler and C. B. Mullins, *J. Chem. Phys.*, 1997, **107**, 10 229.
- 19 Z. L. Wang, T. S. Ahmad and M. A. El-Sayed, *Surf. Sci.*, 1997, **380**, 302.
- 20 Z. L. Wang, J. M. Petroski, T. C. Green and M. A. El-Sayed, *J. Phys. Chem. B*, 1998, **102**, 6145.
- 21 M. Boudart, and G. Djega-Mariadassou, *The Kinetics of Heterogeneous Catalytic Reactions*, Princeton University Press, Princeton, NJ, 1984.